The Rab GTPase Ypt7 is linked to retromer-mediated receptor recycling and fusion at the yeast late endosome

Henning J. kleine Balderhaar[1,*], Henning Arlt[1,*], Clemens Ostrowicz[1], Cornelia Bröcker[1], Frederik Sündermann[2], Roland Brandt[2], Markus Babst[3] and Christian Ungermann[1,‡]

[1]University of Osnabrück, Department of Biology and Chemistry, Biochemistry section, Barbarastrasse 13, 49076 Osnabrück, Germany
[2]University of Osnabrück, Department of Biology and Chemistry, Neurobiology section, Barbarastrasse 11, 49076 Osnabrück, Germany
[3]Department of Biology, University of Utah, Salt Lake City, UT 84112, USA

*These authors contributed equally to this work
‡Author for correspondence (christian.ungermann@biologie.uni-osnabrueck.de)

Accepted 11 August 2010
Journal of Cell Science 123, 4085-4094

doi:10.1242/jcs.071977

Summary

Organelles of the endomembrane system need to counterbalance fission and fusion events to maintain their surface-to-volume ratio. At the late mammalian endosome, the Rab GTPase Rab7 is a major regulator of fusion, whereas the homologous yeast protein Ypt7 seems to be restricted to the vacuole surface. Here, we present evidence that Ypt7 is recruited to and acts on late endosomes, where it affects multiple trafficking reactions. We show that overexpression of Ypt7 results in expansion and massive invagination of the vacuolar membrane, which requires cycling of Ypt7 between GDP- and GTP-bound states. Invaginations are blocked by ESCRT, CORVET and retromer mutants, but not by autophagy or AP-3 mutants. We also show that Ypt7–GTP specifically binds to the retromer cargo-recognition subcomplex, which – like its cargo Vps10 – is found on the vacuole upon Ypt7 overproduction. Our data suggest that Ypt7 functions at the late endosome to coordinate retromer-mediated recycling with the fusion of late endosomes with vacuoles.

Key words: Retromer, Vacuole, Ypt7, HOPS, MVB, Endosome, Vps26

Introduction

Organelles of the endomembrane system are interconnected by vesicular transport, which requires constant fission and fusion reactions at their surface. Whereas fission depends on coat proteins and membrane deformation to generate vesicles, fusion relies on an ordered cascade of tethering and SNARE (soluble NSF attachment protein receptor) complexes to bridge and eventually merge the lipid bilayers. The function of tethering complexes is coordinated by Rab GTPases (Bos et al., 2007). These small Ras-like GTPases are activated by a nucleotide exchange factor (GEF) and interact in their GTP-bound form with their effectors (i.e. tethering complexes). GTPase-activating proteins (GAPs) convert Rabs back to their inactive GDP-bound form (Barr and Lambright, 2010).

In the endocytic pathway, two Rab GTPases coordinate fusion and maturation of endosomes into the late endosome. The Rab5 GTPase Vps21 at the endosome binds the CORVET tethering complex, whereas the Rab7 GTPase Ypt7 interacts with the homologous HOPS complex at the vacuole (Peplowska et al., 2007; Seals et al., 2000). Both tethering complexes consist of six subunits. Four class C subunits (Vps11, Vps16, Vps18 and Vps33) are found in both. In addition, CORVET contains Vps3 and Vps8, and homologous subunits Vps39 and Vps41 are found in the HOPS complex (Nickerson et al., 2009; Peplowska et al., 2007). Vps39 binds to Ypt7 independent of the nucleotide load (Ostrowicz et al., 2010; Wurmser et al., 2000). Several studies indicate that endosomal maturation is connected to the exchange of Rab5 for Rab7 (Poteryaev et al., 2010; Rink et al., 2005; Vonderheit and Helenius, 2005). The maturation process includes the retrieval of receptors via the retromer complex back to the *trans* Golgi network (TGN). The retromer complex consists of two parts: the membrane-remodeling complex contains the BAR domain proteins Vps5 and Vps17, and cooperates with the receptor-binding complex comprising Vps26, Vps29 and Vps35 (Bonifacino and Hurley, 2008; Seaman, 2005). Recent data from mammalian cells indicate that retromer is recruited by Rab7–GTP to late endosomes (Rojas et al., 2008; Seaman et al., 2009). These data suggested the coordination of retrograde transport with the fusion of late endosomes with lysosomes.

As Rab7 GTPase Ypt7 also interacts with the HOPS complex to mediate fusion, we wondered whether we could determine a similar sequence of events in yeast to better understand the regulation of recycling and fusion at the late endosome. Here, we show that Ypt7 overexpression triggers a massive expansion of the vacuole membrane. This expansion is caused by a defect in membrane recycling from late endosomes and increased fusion with the vacuole. Our data indicate that Ypt7 is recruited to late endosomes, interacts with the cargo-recognition complex of retromer, and might have a dual role in membrane recycling and fusion of late endosomes with the vacuole.

Results

Overexpression of Ypt7 causes membrane expansion of the yeast vacuole

We previously presented evidence that the Vps41 subunit of the HOPS tethering complex is recruited to the late endosome (Cabrera et al., 2009; Cabrera et al., 2010). Moreover, Vps41 localization was strongly affected by alterations in Ypt7 (Cabrera et al., 2009), indicating that Ypt7 also might operate at the late endosome. Because Ypt7 deletion results in massive vacuole fragmentation

(Haas et al., 1995), we reasoned that overexpression might provide valuable insights into Ypt7 function at the endosome and vacuole. To our surprise, Ypt7 overproduction resulted in a pronounced change of vacuolar morphology, with the formation of invaginated structures that were further stabilized if the HOPS subunit Vps39 was co-overexpressed (Fig. 1A). If Ypt7 was also GFP tagged, it was found both on the vacuole membrane and partially in the cytoplasm (Fig. 1B), whereas GFP-tagged Ypt7 under the control of the mild *PHO5* promoter localizes to vacuoles and does not affect their morphology (Cabrera et al., 2009). Upon additional overexpression of Vps39, a portion of GFP–Ypt7 was shifted to the vacuole membrane (Fig. 1B, bottom row), consistent with its known interaction with Ypt7 (Wurmser et al., 2000). Regardless of the promoter used for overexpression, the medium or the ploidy of the cells, invaginations of the vacuole membrane were observed (Fig. 1B). These invaginations resulted in the formation of mobile tubular structures within the vacuole lumen (Fig. 1C,D). Similar, although more transient invaginations have been described as autophagic tubules (Binda et al., 2009; Muller et al., 2000). If the observed invaginations bud off into the vacuole lumen, we would expect proteolytic digestion of GFP–Ypt7 to the GFP moiety, as observed for the fate of the autophagy marker GFP–Atg8 (see Fig. 2E, below). This was not the case (Fig. 1E), indicating that the observed expansion is unrelated to (micro-) autophagy.

It was possible that Ypt7 overexpression could alter vacuole morphology by interfering with membrane packaging. We therefore replaced the Ypt7 prenyl anchor with a transmembrane domain (TMD) by homologous recombination, and analyzed vacuole morphology (Fig. 1F). Similar to the previously generated Ypt1 and Sec4 TMD proteins (Ossig et al., 1995), anchoring Ypt7 via a TMD resulted in a functional protein, as judged by the intact vacuole morphology, and led to the same invaginated vacuole

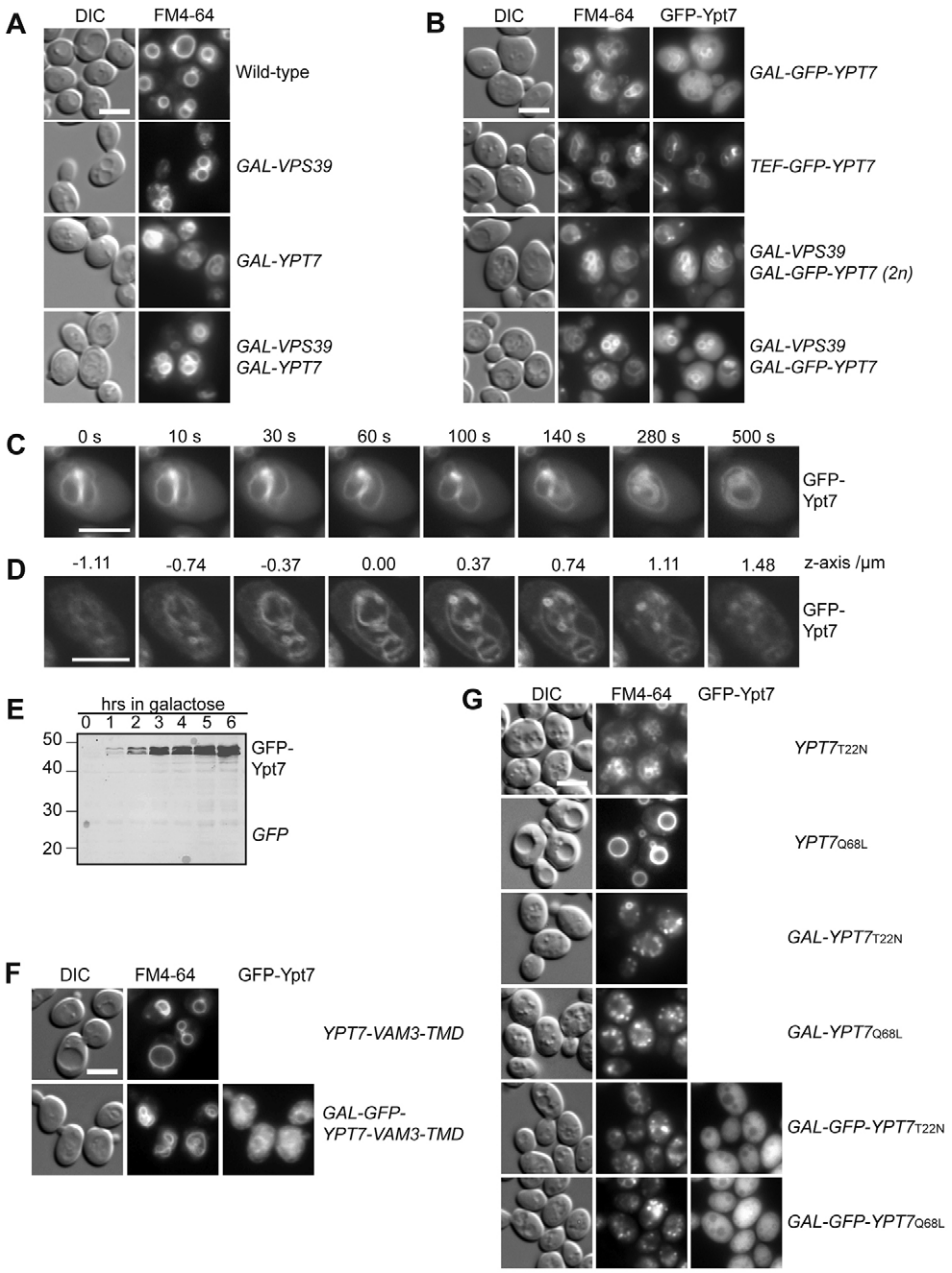

Fig. 1. Ypt7 overproduction induces vacuolar invaginations. (**A**) Ypt7 overproduction causes vacuolar invaginations. Cells with or without *YPT7* and *VPS39* under the control of the *GAL1* promoter (*GAL*) were grown in YPG medium to logarithmic phase, stained with FM4-64, harvested, washed with PBS buffer and analyzed by fluorescence microscopy. Exposure times were kept constant for all mutant strains. (**B**) Ypt7 localization upon overproduction. N-terminally GFP-tagged Ypt7 under the control of the *GAL1* or *TEF1* promoter in haploid or diploid strains (2n). Where indicated, Vps39 was also overproduced. (**C**) Dynamics of the Ypt7-induced vacuolar invaginations. Cells overexpressing GFP–Ypt7 and Vps39 (2n) were grown in YPG overnight, transferred into SGC medium and analyzed for the indicated times by fluorescence microscopy. (**D**) 3D analysis of membrane invaginations. Cells were grown as in C and analyzed by laser-scanning microscopy. (**E**) Stability of GFP–Ypt7 upon overproduction. Cells expressing GFP–Ypt7 from the *GAL1* promoter were grown in YPD overnight and then transferred into YPG to induce expression. 0.5 OD_{600} equivalents of cells were lysed, and proteins were analyzed by SDS-PAGE and western blotting at the indicated time points, using antibodies against GFP. (**F**) Localization of transmembrane-anchored Ypt7. *YPT7* and *GAL1-GFP-YPT7* were C-terminally tagged with the Vam3 transmembrane segment (TMD). Cells were labeled with FM4-64 and analyzed by fluorescence microscopy. (**G**) Expression of *YPT7* nucleotide-locked versions. *YPT7* Q68L or *YPT7* T22N mutants were expressed under the control of the native or *GAL1* promoter. Where indicated, *YPT7* was also GFP tagged. Scale bars (A–D,F,G): 5 µm. DIC, differential interference contrast.

phenotype upon overproduction (Fig. 1F). Ypt7 is, however, no longer restricted to the vacuole, but is found on many membranes in the cell.

Next, we asked whether Ypt7 cycling between GDP and GTP forms is connected to the expansion of the vacuole membrane. Whereas a GDP-locked (T22N) Ypt7 yielded fragmented vacuoles, a GTP-locked (Q68L) version behaved like the wild type (Fig. 1G). However, overexpression of either mutant resulted in vacuole fragmentation, indicating that the altered vacuole morphology phenotype caused by the overexpressed wild-type protein requires cycling of Ypt7 between the GTP and GDP form.

Ypt7 overexpression causes multiple sorting defects

We wondered whether the altered vacuole morphology would perturb sorting or recycling of proteins in the endocytic pathway. Initially, we followed Vps10–GFP, a cargo receptor that transports carboxypeptidase Y (CPY) to the vacuole and is then recycled to the Golgi (Marcusson et al., 1994). In wild-type cells, Vps10 is localized to multiple dots proximal to the vacuole, reflecting most probably Golgi and endosomal structures (Burda et al., 2002), mislocalized to the vacuole in *vps26* deletion mutants (Fig. 2A), and trapped at endosomes if Vps21 and the CORVET subunit Vps8 are upregulated (Markgraf et al., 2009) (Fig. 2A). Interestingly, overexpression of Ypt7 caused a clear shift of Vps10 to the vacuole membrane, suggesting a defect in recycling (Fig. 2A, two lowest panels). We then asked whether the sorting of hydrolases via the endosome would be equally affected. Ypt7 overexpression did not cause any defect in GFP–Cps1 sorting to the vacuole lumen (Fig. 2B), but did perturb CPY sorting, which we followed by analyzing the CPY content in cells (Fig. 2C). This observation is in agreement with the shift of Vps10 to the vacuole under these conditions (Fig. 2A) and its increased proteolytic clipping, which was also observed in *vps26*Δ cells (supplementary material Fig. S1). Strong sorting defects due to Ypt7 overexpression were also detected for AP-3 sorting using a fusion protein of GFP–Nyv1 with a Snc1 transmembrane anchor (GNS construct). In AP-

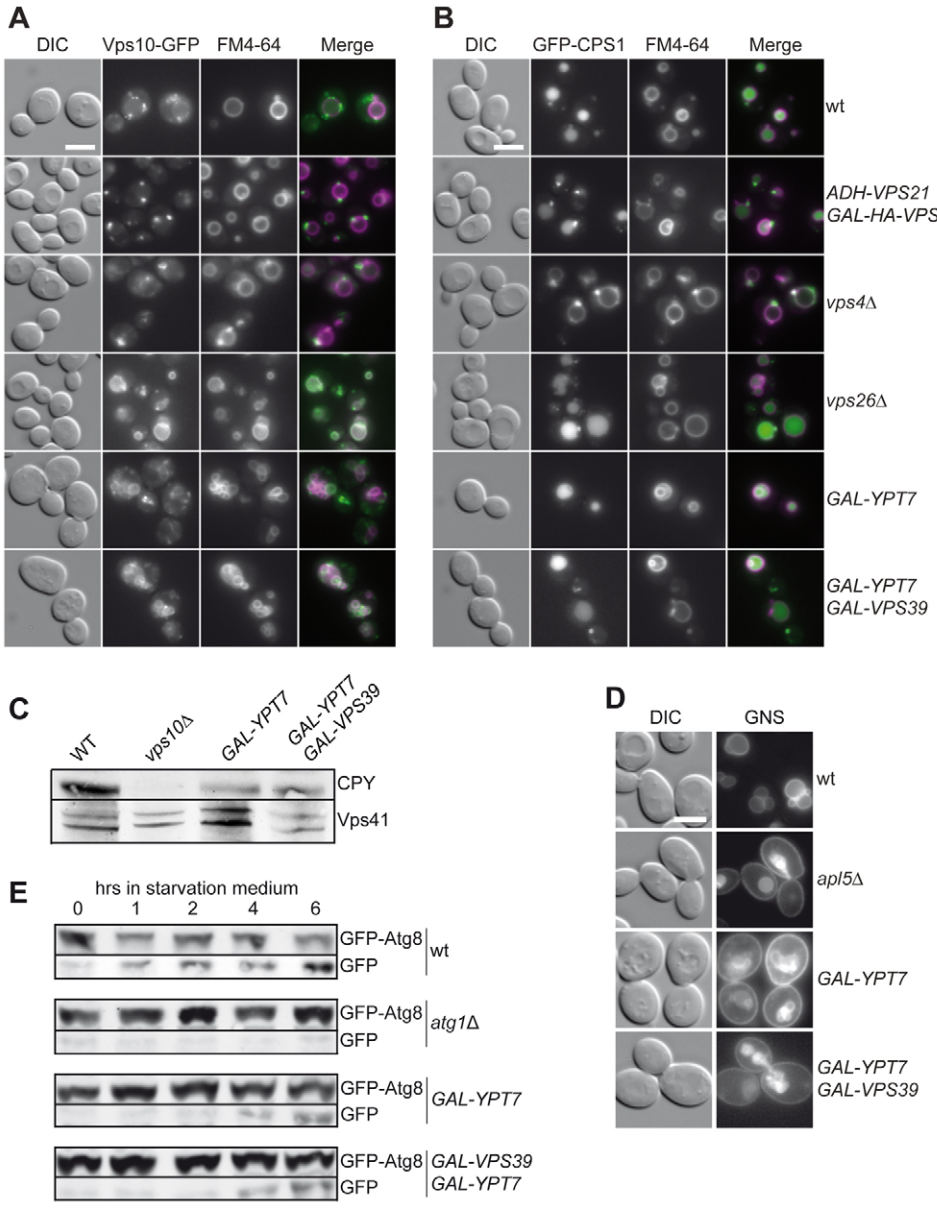

Fig. 2. Overexpression of Ypt7 causes defects in trafficking and autophagy. (**A**) Localization of the GFP-tagged CPY receptor Vps10. *VPS10–GFP* was chromosomally expressed from its native promoter in wild-type cells and indicated mutants. Growth and FM4-64 staining were done as described in Fig. 1A. (**B**) Localization of the biosynthetic cargo protein Cps1 in different trafficking mutants. *GFP–CPS1* was chromosomally expressed from the *PHO5* promoter in the indicated backgrounds. (**C**) Ypt7 overproduction results in CPY secretion. Cells were grown as described in Fig. 1A, 1.5 OD_{600} equivalents of cells were collected by centrifugation, and proteins were analyzed by SDS-PAGE and western blotting using antibodies against CPY and Vps41 (see Markgraf et al., 2009 for details). (**D**) Overproduction of Vps39 and Ypt7 affects the AP-3 pathway. Cells were analyzed by fluorescence microscopy using chimeric protein GFP–Nyv1–Snc1-TMD (GNS), which accumulates at the plasma membrane if the AP-3 pathway is defective (Reggiori et al., 2000). (**E**) Analysis of autophagy. Cells carrying GFP–Atg8 were collected from an exponential growing culture in rich medium (YPG), washed twice with PBS and then resuspended in 10 ml of SD-N medium (2% glucose, 1× YNB without nitrogen). Cells were further incubated at 30°C with agitation. At defined time points, samples (0.8 OD_{600} equivalents of cells) were removed and lysed by alkaline lysis (Markgraf et al., 2009), and proteins were resolved by SDS-PAGE. Full-length GFP–Atg8 and the proteolytic GFP fragment were analyzed by western blotting using antibodies against GFP (Cheong et al., 2005). Scale bars (A,B,D): 5 µm.

3-defective strains, this construct is found on the plasma membrane and is subsequently sorted to the vacuole lumen (Reggiori et al., 2000) (Fig. 2D). Finally, alterations in Ypt7 expression levels caused a clear defect in autophagy, as detected by GFP–Atg8 degradation to free GFP after uptake into the hydrolytic environment of the vacuole lumen (Fig. 2E). We therefore conclude that Ypt7 overexpression not only alters vacuole morphology, but also affects multiple transport events to the vacuole.

A link between Ypt7-mediated alterations of vacuole morphology and endosomal biogenesis

To place the altered vacuole morphology caused by Ypt7 overexpression into the context of trafficking events to the vacuole, we examined morphology in multiple deletion mutants. No effect was observed for several *ATG* mutants, indicating that the observed process is not a consequence of autophagy (Table 1). Mutations in components of the EGO complex, which regulates Tor1 kinase activity (Dubouloz et al., 2005), also showed no effect. More pleiotropic phenotypes were observed for mutants with altered lipid biosynthesis, such as deletions of the phosphoinositide 3-kinase Vps34, the Atg18 lipid-binding protein, the phosphoinositide 3-phosphate-5-kinase Fab1 or enzymes of ergosterol biosynthesis. Some mutants abolished invaginations (*atg18*Δ, *fab1*Δ); others led to vacuole fragmentation (*vps34*Δ) (Table 1).

For three distinct groups of mutants, we observed distinct phenotypes. First, deletions of class D genes such as CORVET subunits *VPS3* and *VPS8* and the Vps21-GEF *VPS9* led to round vacuoles. A similar phenotype was detected for the deletion of the retromer subunit *VPS26* (Fig. 3A). Second, a similar absence of vacuole morphology alterations was observed for class E mutants such as *snf7*Δ, *vps4*Δ or *vps27*Δ, and mutants of ESCRT-associated proteins such as Doa4. However, GFP–Ypt7 was strongly enriched at FM4-64-positive dots proximal to the vacuole, which correspond to class E endosomes (Fig. 3A,B). This is not a mere relocalization of vacuolar proteins, as vacuole-resident proteins such as Vac8 did not accumulate at class E compartments (not shown). Third, deletions of the casein kinase resulted in an enhanced invagination phenotype, with vacuoles reminiscent of large multivesicular bodies (Fig. 3A,B). Thus, Ypt7 is also found at late endosomes and requires endosomal functionality to cause membrane expansion. In agreement with this conclusion, a quantity of Vps41, the HOPS effector subunit, is also localized to class E endosomes (Cabrera et al., 2009; Cabrera et al., 2010).

We further investigated whether the observed invaginated structures would be stable enough to be maintained on isolated vacuoles. Interestingly, vacuoles from wild-type and Ypt7 overexpression strains both showed round vacuoles when isolated (Fig. 3C, inset; supplementary material Fig. S2A). However, quantification of the cross-section area of the vacuoles revealed an up to 50% increase in the surface area of vacuoles from the Ypt7 overexpression strain; this was comparable to the increase caused by deletion of *VPS26* (Fig. 3C). When vacuoles were isolated from cells in which overexpressed Ypt7 was also GFP tagged, we could detect some dots on the vacuolar surface and internal dots in *yck3*Δ cells with overexpressed Ypt7 (supplementary material Fig. S2A). These were absent on vacuoles from retromer mutants. Our data thus reveal that the invaginations of vacuolar membranes seen in vivo are transformed into increased surface area of isolated organelles.

Table 1. Screening of deletion mutants for Ypt7-induced alterations in vacuole morphology

Function	Strain with *GAL1pr-GFP-YPT7*	Vacuole phenotype	GFP–Ypt7 localization
Endosome	*vps3*Δ	Class D	VM[a]
	*vps8*Δ	Class D	VM
	*vps9*Δ	Class D	VM
Retromer	*vps5*Δ	Class B	VM
	*vps17*Δ	Class B	VM
	*vps26*Δ	Class F and A	VM
	*vps29*Δ	Class A	VM
	*vps35*Δ	Class A	VM
ESCRT and MVB	*vps27*Δ	Class E	VM and EC[b]
	*snf7*Δ	Class E	VM and EC
	*vps4*Δ	Class E	VM and EC
	*doa4*Δ	Class E	VM and EC
Vacuole	*yck3*Δ	Invaginated and pinched-off vesicles	VM
	*nyv1*Δ	Class C	VM
	*ccz1*Δ	Class C	VM
Lipid metabolism	*fab1*Δ	Class D	VM
	*vps34*Δ	Class C	VM
	*erg4*Δ	Invaginated	VM
Autophagy	*atg1*Δ	Invaginated	VM
	*atg9*Δ	Invaginated	VM
	*atg18*Δ	Class A and D, no invaginations	VM
	*vtc1*Δ	Invaginated	VM
	*vtc2*Δ	Invaginated (diminished)	VM
	*vtc3*Δ	Invaginated	VM
	*vtc4*Δ	Invaginated	VM
Tor and Ego	*gtr1*Δ	Invaginated	VM
	*gtr2*Δ	Invaginated	VM
	*ego1*Δ	Invaginated	VM
	*ego3*Δ	Invaginated	VM and DA[c]
	*tor1*Δ	Invaginated	VM

Mutants expressing GFP–Ypt7 from the *GAL1* promoter were stained with FM4-64 and analyzed by fluorescence microscopy as described in Fig. 1A.
[a]Accumulation on vacuolar membrane (VM). [b]Accumulation in the class E compartment (EC). [c]Dotted accumulations (DA).

As vacuoles undergo osmotic shock during isolation, we measured the membrane section length in cells to estimate the amount of vacuolar membrane in vivo (Fig. 3D). The membrane length of *vps26*Δ cells increased by 3 µm compared with the wild type and by an additional 2 µm if Ypt7 was overproduced. This shows that the expansion of the vacuole in *YPT7*-overexpressing cells is not solely caused by the retromer recycling defect (Fig. 2C). We ascribe this further expansion (when compared with the *VPS26* deletion) to increased fusion of endosomes with the vacuole (see below). Further quantification shows that the expansion of the vacuole membrane caused by Ypt7 is similar whether or not *VPS26* has been deleted in addition. If we assume that the measured circumference corresponds to a sphere, the increase in surface area would be substantial [from 15.2 (wild type) to 28.7 µm^2 (*vps26*Δ) and 38.5 µm^2 (Ypt7 overexpression)]. Thus, Ypt7-induced expansion is probably the result of a retromer recycling defect in combination with enhanced fusion of endosomes with the vacuole. We note, however, that the deletion of *vps26* also abolishes the invagination phenotype otherwise observed upon Ypt7 overproduction.

Even though Ypt7 was shifted to vacuolar structures by coexpression of Vps39 (Fig. 1A,B), we did not detect any substantial change in membrane expansion (Fig. 3D). Indeed, we did not observe any sizeable change in Ypt7 levels by subcellular fractionation if Vps39 was overexpressed (supplementary material Fig. S2B).

Interaction between retromer and Ypt7

Previous experiments in mammalian cells suggested a direct interaction between Rab7 and retromer (Rojas et al., 2008; Seaman et al., 2009), and our data indicate that the expansion of the vacuole membrane might be the result of reduced membrane recycling. We therefore reasoned that an increase in Ypt7 might favor fusion over recycling at the late endosome, and might shift retromer to the vacuole. To test for Ypt7–retromer interaction, we used GTPγS- or GDP-loaded GST–Vps21 or GST–Ypt7 in a pull-down assay. When a detergent extract from cells expressing HA-tagged Vps26 (a subunit of the cargo-recognition complex) was incubated with GST–Rab proteins, Vps26 was detected on beads loaded with GTPγS (Fig. 4A). Tagging of either retromer subunit yielded a functional protein (supplementary material Fig. S3). Binding to Ypt7–GDP or other GST–Rab proteins was reduced to background levels. We then asked whether this interaction is specific to the cargo-recognition subcomplex of the retromer (consisting of Vps26, Vps29 and Vps35) or the Vps5–Vps17 subcomplex. The interaction of Ypt7–GTPγS with Vps26–HA was robust at higher salt concentrations (supplementary material Fig. S4). Because the two retromer subcomplexes are separated at high salt concentrations (Seaman et al., 1998), this result points towards an interaction between Ypt7 and the cargo-recognition subcomplex. In addition, Vps17–HA binding to Ypt7 was strongly reduced, indicating that Rab binding is specific to the cargo-recognition complex (Fig. 4B). Vps41, a known interaction partner of Ypt7–GTP (Brett et al.,

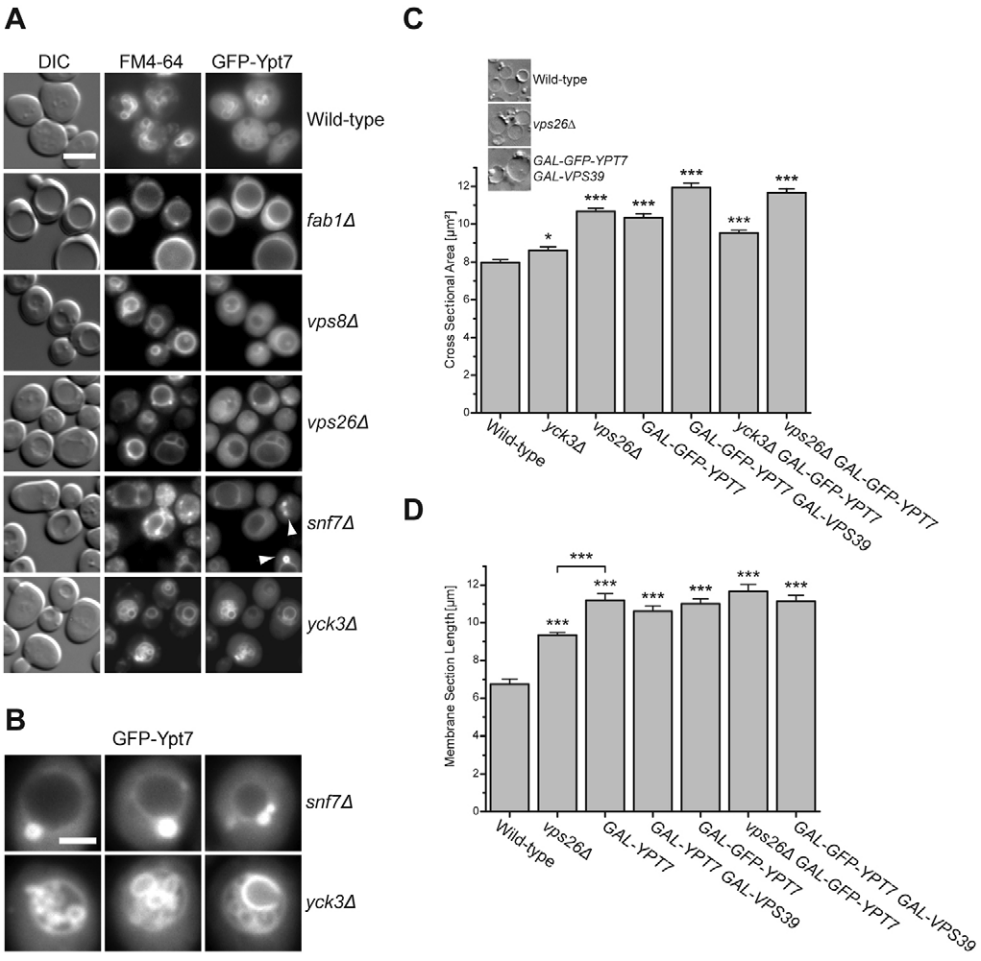

Fig. 3. Deletion of class D and E genes inhibits vacuolar invagination.
(**A**) Morphology of vacuoles in endosomal mutants upon Ypt7 overproduction. Strains that lack the indicated genes and overexpress *GFP–YPT7* were labeled with FM4-64 and analyzed by fluorescence microscopy. Additional mutants are summarized in Table 1. White arrowheads indicate the class E compartments. Scale bar: 5 µm. (**B**) Detailed analysis of GFP–Ypt7 localization in *snf7*Δ and *yck3*Δ cells. Analysis as in A. Scale bar: 2 µm.
(**C**) Invaginations observed in vivo result in increased surface area of isolated vacuoles. Vacuoles from indicated strains were purified and analyzed by microscopy. The cross-section area of the isolated organelles was measured and analyzed as described in the Materials and Methods.
(**D**) Measurement of vacuolar membrane section length in vivo (see Materials and Methods). (C,D) Mean values + s.e.m. Asterisks indicate statistically significant differences compared with wild type: **P*<0.05; ***P*<0.01; ****P*<0.001. Analysis of significance by *t*-test.

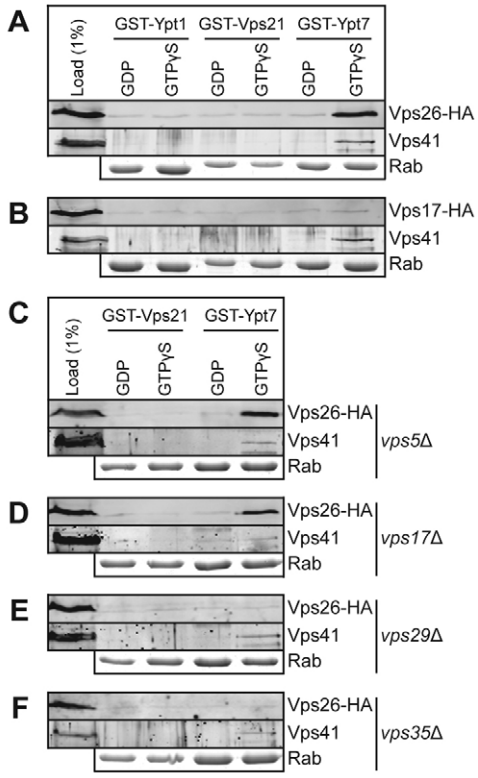

Fig. 4. Ypt7 interacts with retromer. Detergent extracts obtained from cells expressing (**A**) *VPS26–HA* or (**B**) *VPS17–HA* were applied to immobilized GST–Ypt1, GST–Vps21 or GST–Ypt7, which had been preloaded with the indicated nucleotides (all buffers for lysis and washing contained 150 mM NaCl). Bound proteins were eluted, precipitated with TCA and analyzed by western blotting. Beads were then boiled in sample buffer to determine the bound Rab protein in each sample. 8% of the boiled eluate was analyzed by SDS-PAGE and Coomassie staining as a loading control. The interaction of Ypt7–GTPγS with Vps41 was used as a pull-down control. (**C–F**) Ypt7–retromer interaction requires an intact cargo-recognition complex. Pull-down experiment as described in A with lysates from cells expressing *VPS26–HA* in single retromer subunit deletion backgrounds.

2008; Ostrowicz et al., 2010), was retained preferentially on Ypt7–GTPγS in all experiments (Fig. 4). To determine the possible Ypt7-binding partner of the retromer complex, we used deletion mutants of the membrane remodeling complex (*vps5*Δ, *vps17*Δ) and the receptor complex (*vps35*Δ, *vps29*Δ). Binding of Vps26–HA to Ypt7–GTPγS was efficient with *vps5*Δ and *vps17*Δ (Fig. 4C,D), but absent if *vps29*Δ or *vps35*Δ cells were used (Fig. 4E,F), indicating that the intact receptor complex binds Ypt7 (Fig. 4A,C,D).

Colocalization of retromer with the Rab GTPases Vps21 and Ypt7 on endosomes

To follow Ypt7 and the retromer complex in vivo, we constructed functional C-terminal GFP-tagged versions of Vps26 and Vps17 (supplementary material Fig. S3). In wild-type cells, Vps26 and Vps17 are found in multiple dots proximal to the vacuole, which partially colocalize with FM4-64 (Fig. 5A,B). Whereas deletion of *VPS21* resulted in less Vps26–GFP and Vps17–GFP localized to endosomes, colocalization in *ypt7*Δ cells was difficult to assess because of the massive fragmentation of the vacuoles. However, retromer was still detected on endosomal structures in both deletion strains in a subcellular fractionation experiment (Fig. 5C), in contrast to the Rab-dependent localization of mammalian retromer (Rojas et al., 2008; Seaman et al., 2009). This indicates that Rab proteins in yeast are not the sole determinant of retromer localization. Upon Ypt7 overexpression, Vps26–GFP is shifted to vacuoles (Fig. 5A), consistent with the interaction of the receptor complex with Ypt7 (Fig. 4). As yeast late endosomes and vacuoles are poorly resolved by subcellular fractionation, we could not follow this redistribution by subcellular fractionation (not shown).

To investigate the localization of retromer (Vps17–GFP and Vps26–GFP) with endocytic Rab proteins in wild-type cells, we coexpressed them with RFP-tagged Vps21 and Ypt7. Our data indicate that both Rab proteins show partial colocalization with retromer to punctate structures proximal to the vacuole (Fig. 5D,E), which most likely correspond to endosomes. Enlarged images of the vacuole membrane reveal the partial colocalization of Vps21 (or Ypt7) and the retromer subunits. Thus, Ypt7 also functions at the late endosome, consistent with its accumulation in class E compartments (Fig. 3A,B).

We also analyzed whether retromer recruits Ypt7 to the endosomal membrane by analysis of GFP–Ypt7 in different retromer mutants (supplementary material Fig. S5). However, we could not observe any significant differences in the distribution of Ypt7 compared with the wild-type control (see also supplementary material Fig. S2B).

Ypt7 overproduction alters the sensitivity of vacuole fusion to HOPS

To monitor the effect of Ypt7 on fusion, we generated fusion tester strains that overexpressed Ypt7. Fusion was then monitored using vacuoles from two tester strains expressing either the protease Pep4 or its pro-alkaline phosphatase substrate, which is activated by Pep4 after content mixing. Fusion of wild-type vacuoles is insensitive to added HOPS complex, as the endogenous HOPS is already sufficient (Fig. 6A). Furthermore, with increasing HOPS addition, the inhibitory effect of the salt in the buffer reduces fusion significantly. By contrast, vacuoles with excess Ypt7 were clearly stimulated by additional HOPS complex and the inhibitory buffer effect was not observed. These vacuoles fused, however, at a lower rate compared with wild-type vacuoles. We ascribe this to the inefficient sorting of Pho8 by means of the AP-3 pathway, which is defective as a result of Ypt7 overproduction (Fig. 2D).

In summary, we conclude that vacuoles with excess Ypt7 can fuse efficiently and will be readily stimulated by available HOPS complex. Even though we analyzed vacuole fusion, a similar effect might apply to the late endosome, where Ypt7 also functions (Fig. 3, Fig. 5D,E). This would explain the preference for fusion over retrieval at the late endosome, as observed for the relocalization of the retromer complex to vacuoles.

Discussion

We analyzed the role of Ypt7 at the late endosome to vacuole transition. Like its Rab7 homolog, Ypt7 might be involved in both receptor recycling and HOPS-mediated vacuole fusion. To analyze Ypt7 function, we followed the consequences of Ypt7 overexpression for protein sorting and vacuole morphology. We observed a massive expansion of the vacuole membrane, which leads to a dramatic increase in surface area. We ascribe this to increased fusion of endosomes with vacuoles at the expense of efficient recycling (Fig. 2, Fig. 6A). In agreement with this

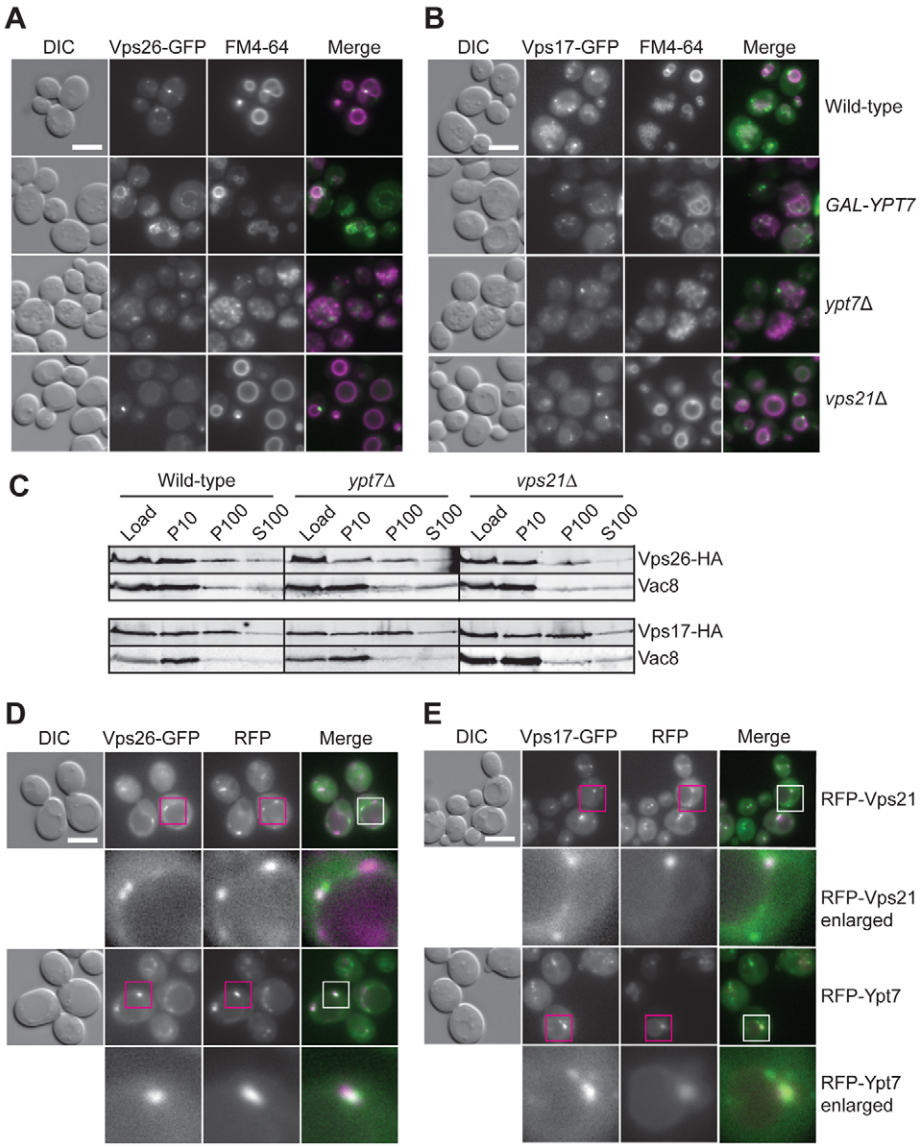

Fig. 5. Colocalization of retromer with the Rab proteins Vps21 and Ypt7 on endosomes. (**A**,**B**) Localization of retromer subunits Vps26–GFP (A) and Vps17–GFP (B) in the wild type, with overexpressed Ypt7 or in Rab deletion strains. Cells were grown in YPG medium to logarithmic phase. Staining with FM4-64 as described in Fig. 1A. Scale bars: 5 µm. (**C**) Subcellular distribution of Vps26–HA in the wild type, and *YPT7* and *VPS21* deletion backgrounds. Lysed spheroplasts were fractionated by centrifugation, resulting in a 10,000 ***g*** pellet (P10), a 100,000 ***g*** pellet (P100) and a final supernatant (S100). Fractions were analyzed by western blotting using antibodies against HA and Vac8 as a vacuolar marker protein. (**D**,**E**) Colocalization of the Rab GTPases Ypt7 and Vps21 with retromer subunits. Plasmids encoding N-terminally RFP-tagged Rab proteins were transformed into strains with Vps26–GFP (D) or Vps17–GFP (E). Cells were grown to logarithmic phase in synthetic medium (SDC) without tryptophan for maintenance of plasmids. Detailed views of the colocalization are shown (enlarged boxed regions). Scale bars (A,B,D,E): 5 µm.

interpretation, retromer and its cargo Vps10 are shifted to the vacuole membrane. Indeed, retromer is able to bind Ypt7–GTP through its cargo-recognition subcomplex, consisting of Vps26–Vps29–Vps35, as observed for mammalian cells (Rojas et al., 2008). Our data also revealed colocalization of retromer and Ypt7 in wild-type cells and substantial accumulation of Ypt7 at immature class E late endosomes. This suggests that Ypt7 function at the late endosome is regulated directly or indirectly by ESCRT, and is tightly linked to the maturation state of the organelle. We suggest that Ypt7 overexpression overrides this regulation, resulting in membrane expansion of the vacuole. As Ypt7 also interacts with retromer (Figs 4, 5), we postulate that there is cross-talk between retromer, ESCRT and the fusion machinery through Ypt7.

Our data confirm that Ypt7 affects retromer functionality, similar to the observation made in mammalian cells for Rab7 and retromer (Rojas et al., 2008; Seaman et al., 2009). In contrast to mammalian cells, we did not find that the membrane localization of retromer was affected by Ypt7 deletion. This is expected, because the Vps26–Vps29–Vps35 cargo-recognition complex also cooperates with several sorting nexins, such as Snx3, for receptor retrieval at the early endosome (Strochlic et al., 2008; Strochlic et al., 2007). However, the strong interaction of Ypt7–GTP with retromer is restricted to the Vps26–Vps29–Vps35 subcomplex, although we could not identify the direct binding partner. As a consequence of Ypt7-mediated membrane fusion, vacuoles expand and retromer shifts to the vacuole surface. We do not currently know whether this is a direct consequence of Ypt7 binding or is due to enhanced consumption of late endosomes. As retromer might function inefficiently at the vacuole, membrane recycling might be equally affected. Our data would thus suggest that Ypt7 coordinates membrane recycling and fusion at the late endosome.

Ypt7 was previously found primarily on vacuoles. During our analysis of mutants with altered vacuole morphology due to Ypt7 overexpression, two classes showed a substantial decrease in vacuolar invaginations. In class D mutants, Ypt7 localized normally to membranes and the vacuole morphology was normal (class D) (Table 1). Class D vacuoles have endosome and vacuolar properties, and are deficient in membrane dynamics in events such as inheritance, fragmentation and ESCRT-mediated multivesicular body (MVB) formation (Peplowska et al., 2007; Takeda et al.,

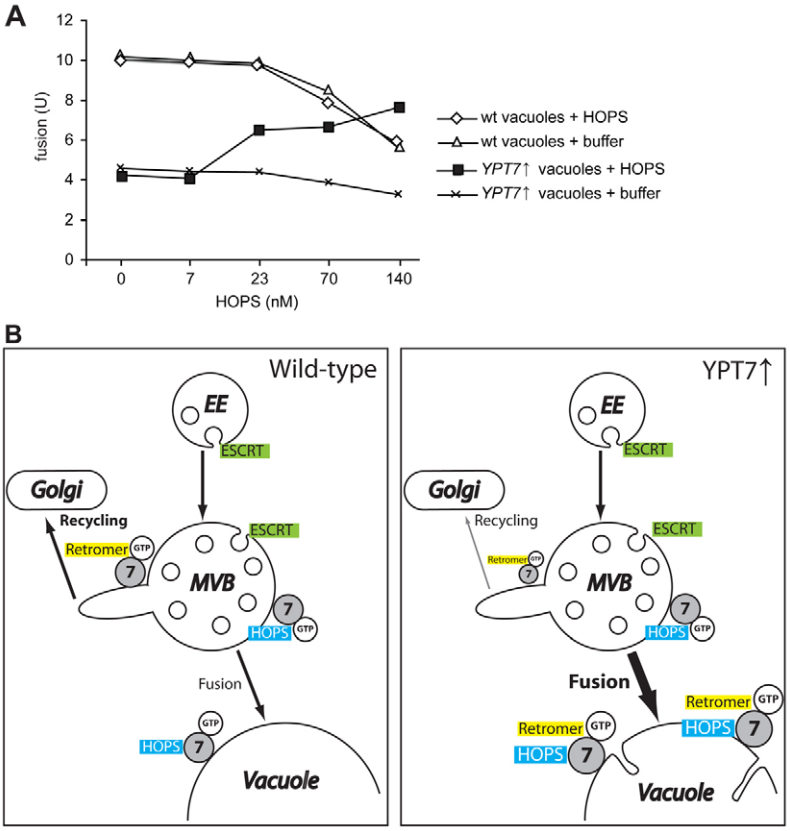

Fig. 6. Effect of Ypt7 overexpression on vacuole fusion. (**A**) HOPS stimulates fusion of vacuoles carrying an excess of Ypt7. Vacuoles were isolated from wild-type BJ3505 (*pep4*Δ) and DKY6281 (*pho8*Δ) strains or from BJ3505 (*pep4*Δ, *GPD1-YPT7*) and DKY6281 (*pho8*Δ, *GPD1-YPT7*) strains as described (Cabrera and Ungermann, 2008; Haas, 1995). The fusion reaction was performed in fusion reaction buffer (150 mM KCl, 5 mM $MgCl_2$, 20 mM sorbitol, 1 mM PIPES-KOH pH 6.8) containing ATP-regenerating system, 1 ng Sec18, 10 µM CoA and 1 mM GTP. Each fusion reaction contains 3 µg of each vacuole type. The reactions were supplemented with the indicated amount of purified HOPS or the purification buffer (Ostrowicz et al., 2010). After incubation for 90 minutes at 26°C, the reactions were developed for 5 minutes at 30°C and the OD_{400} was measured (LaGrassa and Ungermann, 2005). (**B**) Model of the effect of Ypt7 on vacuole morphology. In wild-type cells (left), Ypt7 function is balanced between its role in retromer-mediated recycling of cargo receptors and HOPS-controlled fusion with the vacuole. Upon YPT7 overproduction (right), fusion is favored over recycling and retromer is shifted to the vacuole. EE, early endosome; 7, Ypt7.

2008). Similarly, deletions of ESCRT subunits and *DOA4*, which result in the expanded class E endosome close to the vacuole, show no invaginations. However, overexpressed Ypt7 is strongly enriched in dots at the late endosome (Fig. 3B). Class E mutants also show a partial defect in the recycling of Vps10 and retromer subunits accumulate in the class E compartment (Babst et al., 1997; Seaman et al., 1998). This suggests that ESCRT function precedes retromer activity at the late endosome. Ypt7 might have a role in staging these processes, because overexpression of this Rab GTPase bypasses these steps and results in premature fusion. We present a model in which the maturation of the endosome is linked to sequential activity of ESCRT, retromer and the fusion machinery, with Ypt7–GTP as a central regulator (Fig. 6B). We believe that maturation requires not only Ypt7 activation, but also coordination between ESCRT-mediated downregulation and retromer-driven recycling. If Ypt7 is in excess, fusion is favored, and might bypass ESCRT- and retromer-mediated control. Indeed, the vacuole membrane surface area more than doubles if Ypt7 is overproduced even in *vps26*Δ cells (Fig. 3D), although the invagination phenotype is lost (discussed below). In wild-type cells, a possible signal for the maturation state of the endosome could be ubiquitylated cargo. In agreement with this, mutants in ESCRT can be bypassed if the remaining membrane-bound ubiquitin is shielded and/or removed (Luhtala and Odorizzi, 2004). Potentially, Ypt7 would be activated prior to endosomal maturation, interact with retromer to allow receptor recycling and only bind to HOPS once ubiquitin has been removed. Such a control might be absent if Ypt7 is overproduced. How this coordination is mediated, and whether ubiquitin is indeed the signal, remains a major question for future analyses.

Previously, a defect in recycling was linked to the surface expansion of vacuoles. Indeed, mutants defective in phosphoinositide-3,5-bisphosphate synthesis or turnover have large round vacuoles (Bonangelino et al., 2002; Gary et al., 1998). However, for Ypt7 overexpression mutants, we observed massive vacuolar invaginations in vivo, which expand into large vacuoles when isolated (Fig. 3C). This indicates that the invagination of the surface could be caused by stabilization of negatively curved membranes. We previously identified the Ypt7-effector subunit Vps41, a component of the HOPS complex, as a target of the casein kinase Yck3 (Cabrera et al., 2009; Cabrera et al., 2010; LaGrassa and Ungermann, 2005). Vps41 mutants strongly accumulate on vacuolar surfaces if Ypt7 is upregulated (Cabrera et al., 2009). We therefore propose that either Vps41 itself or components of or associated with the HOPS complex are involved in stabilizing the altered vacuolar morphology. Indeed, overexpression of Ypt7 in *yck3*Δ mutants results in even deeper invaginations, which are maintained in isolated vacuoles (Fig. 3B,C; supplementary material Fig. S3). In agreement with these speculations, Wickner and colleagues reported that liposomes, which fused in a HOPS-dependent reaction, showed massive invagination (Mima and Wickner, 2009). We therefore postulate that HOPS contributes to the alteration in the vacuolar membrane observed here. If ESCRT or retromer are lacking, fusion is still favored (Fig. 3D), but membrane-active proteins (potentially HOPS) might not be stabilized nor remain active at the vacuole, and the membrane invagination phenotype is lost.

Our data also show that HOPS subunit Vps39 affects the intracellular localization of Ypt7. Vps39 binds to all forms of Ypt7 (Wurmser et al., 2000) and can cluster Ypt7 at endosomal structures (Ostrowicz et al., 2010). However, Vps39 does not enhance the Ypt7-triggered vacuole surface expansion (Fig. 3D). How Vps39 stimulates Ypt7 clustering is so far unknown.

Our data are consistent with the idea that the endosomal membrane contains microdomains responsible for recycling, downregulation or sorting (Seaman, 2009). We term these structures suborganellar microcompartments, as a more general name to distinguish them from the terminology used for the plasma membrane (Lingwood and Simons, 2010). In the case of Ypt7 overexpression, the balance between these microcompartments is shifted and results in pronounced fusion. How such regulation is mediated at endosomes in wild-type cells will be the focus of future studies.

Materials and Methods

Yeast strains and plasmids

Saccharomyces cerevisiae strains used in this study are listed in supplementary material Table S1. Gene deletion and tagging were done by homologous recombination of PCR fragments. Overexpression of *YPT7* or *VPS39* with the *GAL1* promoter was carried out by integrating a PCR product with flanking regions of the respective gene, amplified from pFA6a-*kanMX6-PGAL1*, pFA6a-*HIS3MX6-PGAL1*, pFA6a-*HIS3MX6-PGAL1-GFP* and pFA6a-*TRP1-PGAL1-GFP* (Longtine et al., 1998). *VPS10* was tagged at the C terminus by amplification of a gene cassette from pFA6a-*GFP*(S65T)-*kanMX6* with flanking regions of *VPS10*. *VPS39 and YPT7* were placed under the control of the *GPD1* or *TEF1* promoter and *TEF1pr-yeGFP* by amplifying cassettes from pYM-N18, pYM-N19 and pYM-N21 with flanking regions of the respective genes (Janke et al., 2004). *VPS17* and *VPS26* were tagged at their C termini with 3×HA, GFP or the TAP tag by PCR amplification from plasmids pYM25 (yeGFP), pYM24 (3×HA) and pYM TAP-natNT2 with the respective flanking sequences (Janke et al., 2004). N-terminal tagging with *PHO5pr-GFP-CPS1* was performed as described (Markgraf et al., 2009). Plasmids pGNS416 expressing *GFP-NYV1-SNC1* and pCu-*GFP-ATG8* were kind gifts from Fulvio Reggiori (University Medical Center Utrecht, The Netherlands). The N-terminal RFP-tagged versions of Vps21 and Ypt7 were generated by amplification of the genes from genomic DNA, digestion with *Bam*HI and *Sac*I, and insertion into the *Bam*HI and *Sac*I sites of a pV2 plasmid (CEN, *PHO5pr*) that carries DsRed from a pRSET-B DsRed dimer (Markgraf et al., 2009)

C-terminal tagging of *YPT7* (without the C-terminal cysteine residues) with the transmembrane domain of Vam3 was carried out by integration of a PCR product made with the plasmid pKS133-6 pFA6-hphNT1 and primers S1 (GACTATAATGATGCCATCAATATTCGCCTAGATGGAGAAAATAATTCTAAGGTCACCCTAATCATTATAATAGTTGTGTGCATGGTGGTATTGCTTGCTG) and S2 (CGCTATAAAGGATTACATAATAGAAGATACAATTAAGTAGTACAGCTCAATCGATGAATTCGAGCTCG).

Fluorescence and laser-scanning microscopy

Cells carrying a GFP or RFP tag were grown to logarithmic phase in yeast extract peptone medium (YP) containing 2% glucose or galactose, respectively. For maintenance of plasmids, cells were grown in synthetic medium supplemented with essential amino acids (SDC). Staining of yeast vacuoles with the lipophilic dye FM4-64 was done as described (LaGrassa and Ungermann, 2005). Grown cells were collected by centrifugation, washed once with 1 ml PBS buffer and mounted on a cover slide for microscopy. Images were acquired using a Leica DM5500 microscope (Leica, Mannheim, Germany) with a SPOT Pursuit-XS camera (Diagnostic Instruments, Sterling Heights, MI, USA) using filters for GFP, RFP and FM4-64. Laser-scanning microscopy was performed using a LSM 510 Meta (Carl Zeiss MicroImaging, Jena, Germany). GFP signals were followed using an argon laser (6A, 488 nm and 6% intensity). Pictures were processed using Adobe Photoshop 10 (Adobe Systems, Munich, Germany), AxioVision (Zeiss Imaging Solutions, Hallbergmoos, Germany) and ImageJ (developed by Wayne Rasband, National Institutes of Health, Bethesda, MD, USA).

In vivo quantification of vacuolar membrane

Cultures were stained with lipophilic dye FM4-64 and analyzed by fluorescence microscopy as described above. For each strain, *z*-stacks of approximately six random fields were taken (16 slices per stack; 0.2 µm intervals). To achieve better resolution of the intravesicular structures and the vacuolar circumferences, each data set was subjected to a 3D deconvolution using AutoQuant X (Media Cybernetics, Bethesda, MD, USA). The lengths of the outer vacuolar membrane and invaginations inside the organelle (n>75) were determined in three different planes (for each measurement) using a self-written plug-in for ImageJ (see supplementary material Fig. S6). Statistical analysis of P values was performed using the t test (Origin software, OriginLab, Northampton, MA, USA) and additionally verified with a bootstrapping algorithm applied to each data set.

Glutathione–Rab pull down

The glutathione–Rab pull-down experiment was done as described (Markgraf et al., 2009). Briefly, recombinant GST fusion proteins (300 µg) were loaded with GDP or GTPγS. Rab proteins were coupled to GSH beads. Yeast cells were lysed by extensive centrifugation with glass beads for 2 × 10 minutes at 4°C in lysis buffer [50 mM HEPES/KOH pH 7.4, 0.15% NP-40 (Igepal CA-630; Sigma, Munich, Germany) with 300 mM or 150 mM NaCl as indicated]. Lysate was cleared by centrifugation at 20,000 ***g***. 250 OD_{600} equivalents of cleared lysate were added to the beads, followed by incubation for 1 hour at 4°C on a rotating wheel. Beads were washed three times with buffer (150 mM or 300 mM NaCl, as indicated in the figure legends) and proteins were eluted with 20 mM EDTA. Eluates were precipitated with trichloracetic acid (TCA), and analyzed by SDS-PAGE and western blotting. Bound GST–Rab was eluted from the beads by boiling in sample buffer, and analyzed by SDS PAGE and Coomassie staining as a Rab loading control.

Total protein extraction from yeast cells

Yeast protein extracts were obtained from indicated strains, grown in appropriate medium, as indicated in the corresponding figure legends. Equivalent amounts of cells were lysed in 0.25 M NaOH, 140 mM β-mercaptoethanol and 3 mM PMSF. Samples were incubated on ice for 10 minutes and subsequently precipitated with TCA (13% final concentration). After a washing step with acetone, the protein pellet was resuspended in SDS sample buffer. Equal amounts of protein were analyzed by SDS-PAGE and western blotting. To follow the degradation of the Vps10–GFP fusion protein, cycloheximide was added to cultures in mid-logarithmic phase in a concentration of 50 µg/ml. Samples were taken at the indicated time points and lysed as described above.

Biochemical fractionation of yeast cells

Fractionation was done as described (LaGrassa and Ungermann, 2005). Briefly, yeast cell were lysed and centrifuged for 15 minutes at 10,000 ***g*** at 4°C. The supernatant was then centrifuged for 1 hour at 100,000 ***g***, resulting in a P100 pellet and a S100 supernatant fraction. The S100 fraction was TCA precipitated, the pellet was acetone washed and, as the P10 and P100 pellet, resuspended in SDS sample buffer. Proteins were subsequently analyzed by SDS-PAGE and western blotting.

Isolation and statistical analysis of yeast vacuoles

Vacuoles were isolated by DEAE-dextran lysis of cells and Ficoll density gradient flotation (Haas, 1995), and immediately analyzed by fluorescence microscopy. Measurement of the cross-section area was performed using ImageJ. Descriptive analysis (Origin software) was applied to each data set (190<n<250).

We thank Fulvio Reggiori for discussions and plasmids, Siegfried Engelbrecht-Vandré for comments, and Achim Paululat (University of Osnabrück) for sharing the laser-scanning microscope. This work was supported by the SFB431, the DAAD and the Hans-Mühlenhoff foundation (to C.U.).

Supplementary material available online at
http://jcs.biologists.org/cgi/content/full/123/23/4085/DC1

References

Babst, M., Sato, T. K., Banta, L. M. and Emr, S. D. (1997). Endosomal transport function in yeast requires a novel AAA-type ATPase, Vps4p. *EMBO J.* **16**, 1820-1831.

Barr, F. and Lambright, D. G. (2010). Rab GEFs and GAPs. *Curr. Opin. Cell Biol.* **22**, 461-470.

Binda, M., Peli-Gulli, M. P., Bonfils, G., Panchaud, N., Urban, J., Sturgill, T. W., Loewith, R. and De Virgilio, C. (2009). The Vam6 GEF controls TORC1 by activating the EGO complex. *Mol. Cell* **35**, 563-573.

Bonangelino, C. J., Nau, J. J., Duex, J. E., Brinkman, M., Wurmser, A. E., Gary, J. D., Emr, S. D. and Weisman, L. S. (2002). Osmotic stress-induced increase of phosphatidylinositol 3,5-bisphosphate requires Vac14p, an activator of the lipid kinase Fab1p. *J. Cell Biol.* **156**, 1015-1028.

Bonifacino, J. S. and Hurley, J. H. (2008). Retromer. *Curr. Opin. Cell Biol.* **20**, 427-436.

Bos, J. L., Rehmann, H. and Wittinghofer, A. (2007). GEFs and GAPs: critical elements in the control of small G proteins. *Cell* **129**, 865-877.

Brett, C. L., Plemel, R. L., Lobinger, B. T., Vignali, M., Fields, S. and Merz, A. J. (2008). Efficient termination of vacuolar Rab GTPase signaling requires coordinated action by a GAP and a protein kinase. *J. Cell Biol.* **182**, 1141-1151.

Burda, P., Padilla, S. M., Sarkar, S. and Emr, S. D. (2002). Retromer function in endosome-to-Golgi retrograde transport is regulated by the yeast Vps34 PtdIns 3-kinase. *J. Cell Sci.* **115**, 3889-3900.

Cabrera, M. and Ungermann, C. (2008). Purification and in vitro analysis of yeast vacuoles. *Methods Enzymol.* **451**, 177-196.

Cabrera, M., Langemeyer, L., Mari, M., Rethmeier, R., Orban, I., Perz, A., Bröcker, C., Griffith, J., Klose, D., Steinhoff, H. J. et al. (2010). Phosphorylation of a membrane curvature-sensing motif switches function of the HOPS subunit Vps41 in membrane tethering. *J. Cell Biol*. in press.

Cabrera, M., Ostrowicz, C. W., Mari, M., LaGrassa, T. J., Reggiori, F. and Ungermann, C. (2009). Vps41 phosphorylation and the Rab Ypt7 control the targeting of the HOPS complex to endosome-vacuole fusion sites. *Mol. Biol. Cell* **20**, 1937-1948.

Cheong, H., Yorimitsu, T., Reggiori, F., Legakis, J. E., Wang, C. W. and Klionsky, D. J. (2005). Atg17 regulates the magnitude of the autophagic response. *Mol. Biol. Cell* **16**, 3438-3453.

Dubouloz, F., Deloche, O., Wanke, V., Cameroni, E. and De Virgilio, C. (2005). The TOR and EGO protein complexes orchestrate microautophagy in yeast. *Mol. Cell* **19**, 15-26.

Eitzen, G., Will, E., Gallwitz, D., Haas, A. and Wickner, W. (2000). Sequential action of two GTPases to promote vacuole docking and fusion. *EMBO J.* **19**, 6713-6720.

Gary, J. D., Wurmser, A. E., Bonangelino, C. J., Weisman, L. S. and Emr, S. D. (1998). Fab1p is essential for PtdIns(3)P 5-kinase activity and the maintenance of vacuolar size and membrane homeostasis. *J. Cell Biol.* **143**, 65-79.

Haas, A. (1995). A quantitative assay to measure homotypic vacuole fusion in vitro. *Methods Cell Sci.* **17**, 283-294.

Haas, A., Scheglmann, D., Lazar, T., Gallwitz, D. and Wickner, W. (1995). The GTPase Ypt7p of *Saccharomyces cerevisiae* is required on both partner vacuoles for the homotypic fusion step of vacuole inheritance. *EMBO J.* **14**, 5258-5270.

Janke, C., Magiera, M. M., Rathfelder, N., Taxis, C., Reber, S., Maekawa, H., Moreno-Borchart, A., Doenges, G., Schwob, E., Schiebel, E. et al. (2004). A versatile toolbox for PCR-based tagging of yeast genes: new fluorescent proteins, more markers and promoter substitution cassettes. *Yeast* **21**, 947-962.

LaGrassa, T. J. and Ungermann, C. (2005). The vacuolar kinase Yck3 maintains organelle fragmentation by regulating the HOPS tethering complex. *J. Cell Biol.* **168**, 401-414.

Lingwood, D. and Simons, K. (2010). Lipid rafts as a membrane-organizing principle. *Science* **327**, 46-50.

Longtine, M. S., McKenzie, A., 3rd, Demarini, D. J., Shah, N. G., Wach, A., Brachat, A., Philippsen, P. and Pringle, J. R. (1998). Additional modules for versatile and economical PCR-based gene deletion and modification in *Saccharomyces cerevisiae*. *Yeast* **14**, 953-961.

Luhtala, N. and Odorizzi, G. (2004). Bro1 coordinates deubiquitination in the multivesicular body pathway by recruiting Doa4 to endosomes. *J. Cell Biol.* **166**, 717-729.

Marcusson, E. G., Horazdovsky, B. F., Cereghino, J. L., Gharakhanian, E. and Emr, S. D. (1994). The sorting receptor for yeast vacuolar carboxypeptidase Y is encoded by the VPS10 gene. *Cell* **77**, 579-586.

Markgraf, D. F., Ahnert, F., Arlt, H., Mari, M., Peplowska, K., Epp, N., Griffith, J., Reggiori, F. and Ungermann, C. (2009). The CORVET subunit Vps8 cooperates with the Rab5 homolog Vps21 to induce clustering of late endosomal compartments. *Mol. Biol. Cell* **20**, 5276-5289.

Mima, J. and Wickner, W. (2009). Phosphoinositides and SNARE chaperones synergistically assemble and remodel SNARE complexes for membrane fusion. *Proc. Natl. Acad. Sci. USA* **106**, 16191-16196.

Muller, O., Sattler, T., Flotenmeyer, M., Schwarz, H., Plattner, H. and Mayer, A. (2000). Autophagic tubes. Vacuolar invaginations involved in lateral membrane sorting and inverse vesicle budding. *J. Cell Biol.* **151**, 519-528.

Nickerson, D. P., Brett, C. L. and Merz, A. J. (2009). Vps-C complexes: gatekeepers of endolysosomal traffic. *Curr. Opin. Cell Biol.* **21**, 543-551.

Ossig, R., Laufer, W., Schmitt, H. D. and Gallwitz, D. (1995). Functionality and specific membrane localization of transport GTPases carrying C-terminal membrane anchors of synaptobrevin-like proteins. *EMBO J.* **14**, 3645-3653.

Ostrowicz, C. W., Brocker, C., Ahnert, F., Nordmann, M., Lachmann, J., Peplowska, K., Perz, A., Auffarth, K., Engelbrecht-Vandre, S. and Ungermann, C. (2010). Defined subunit arrangement and Rab interactions are required for functionality of the HOPS tethering complex. *Traffic* **11**, 1334-1346.

Peplowska, K., Markgraf, D. F., Ostrowicz, C. W., Bange, G. and Ungermann, C. (2007). The CORVET tethering complex interacts with the yeast Rab5 homolog Vps21 and is involved in endo-lysosomal biogenesis. *Dev. Cell* **12**, 739-750.

Poteryaev, D., Datta, S., Ackema, K., Zerial, M. and Spang, A. (2010). Identification of the switch in early-to-late endosome transition. *Cell* **141**, 497-508.

Reggiori, F., Black, M. W. and Pelham, H. R. (2000). Polar transmembrane domains target proteins to the interior of the yeast vacuole. *Mol. Biol. Cell* **11**, 3737-3749.

Rink, J., Ghigo, E., Kalaidzidis, Y. and Zerial, M. (2005). Rab conversion as a mechanism of progression from early to late endosomes. *Cell* **122**, 735-749.

Rojas, R., van Vlijmen, T., Mardones, G. A., Prabhu, Y., Rojas, A. L., Mohammed, S., Heck, A. J., Raposo, G., van der Sluijs, P. and Bonifacino, J. S. (2008). Regulation of retromer recruitment to endosomes by sequential action of Rab5 and Rab7. *J. Cell Biol.* **183**, 513-526.

Seals, D. F., Eitzen, G., Margolis, N., Wickner, W. T. and Price, A. (2000). A Ypt/Rab effector complex containing the Sec1 homolog Vps33p is required for homotypic vacuole fusion. *Proc. Natl. Acad. Sci. USA* **97**, 9402-9407.

Seaman, M. N. (2005). Recycle your receptors with retromer. *Trends Cell Biol.* **15**, 68-75.

Seaman, M. N. (2009). Enhanced SnapShot: endosome-to-Golgi retrieval. *Cell* **139**, 1198.

Seaman, M. N., McCaffery, J. M. and Emr, S. D. (1998). A membrane coat complex essential for endosome-to-Golgi retrograde transport in yeast. *J. Cell Biol.* **142**, 665-681.

Seaman, M. N., Harbour, M. E., Tattersall, D., Read, E. and Bright, N. (2009). Membrane recruitment of the cargo-selective retromer subcomplex is catalysed by the small GTPase Rab7 and inhibited by the Rab-GAP TBC1D5. *J. Cell Sci.* **122**, 2371-2382.

Strochlic, T. I., Setty, T. G., Sitaram, A. and Burd, C. G. (2007). Grd19/Snx3p functions as a cargo-specific adapter for retromer-dependent endocytic recycling. *J. Cell Biol.* **177**, 115-125.

Strochlic, T. I., Schmiedekamp, B. C., Lee, J., Katzmann, D. J. and Burd, C. G. (2008). Opposing activities of the Snx3-retromer complex and ESCRT proteins mediate regulated cargo sorting at a common endosome. *Mol. Biol. Cell* **19**, 4694-4706.

Takeda, K., Cabrera, M., Rohde, J., Bausch, D., Jensen, O. N. and Ungermann, C. (2008). The vacuolar V(1)/V(0)-ATPase is involved in the release of the HOPS subunit Vps41 from vacuoles, vacuole fragmentation and fusion. *FEBS Lett.* **582**, 1558-1563.

Vonderheit, A. and Helenius, A. (2005). Rab7 associates with early endosomes to mediate sorting and transport of Semliki forest virus to late endosomes. *PLoS Biol.* **3**, e233.

Wurmser, A. E., Sato, T. K. and Emr, S. D. (2000). New component of the vacuolar class C-Vps complex couples nucleotide exchange on the Ypt7 GTPase to SNARE-dependent docking and fusion. *J. Cell Biol.* **151**, 551-562.